

Mechanics from Calorimetry: A New Probe of Elasticity for Responsive Hydrogels

Frank J. Aangenendt,^{1,2,3} Johan Mattsson,⁴ Wouter G. Ellenbroek,^{2,5} and Hans M. Wyss^{1,2,3,*}

¹*Dutch Polymer Institute (DPI), P.O. Box 902, 5600AX Eindhoven, The Netherlands*

²*Institute for Complex Molecular Systems, Eindhoven University of Technology, Eindhoven, The Netherlands*

³*Department of Mechanical Engineering, Materials Technology,
Eindhoven University of Technology, Eindhoven, The Netherlands*

⁴*School of Physics and Astronomy, University of Leeds, Leeds LS2 9JT, U.K.*

⁵*Department of Physics, Eindhoven University of Technology, Eindhoven, The Netherlands*

(Dated: August 3, 2022)

Hydrogels based on polymers such as poly-N-isopropylacrylamide (pNIPAM) undergo a volume phase transition in response to changes in temperature. During this transition, distinct changes in both thermal and mechanical properties are observed. Here we illustrate and exploit the inherent thermodynamic link between thermal and mechanical properties by showing that the compressive elastic modulus of pNIPAM hydrogels can be determined using differential scanning calorimetry (DSC). We verify this by using conventional osmotic compression tests. Our method should be particularly valuable for determining the mechanical response of submicron-sized and/or oddly shaped particles, which is not readily accessible using standard methods.

PACS numbers: 83.80.Kn, 81.70.Pg, 65.60.+a, 62.20.de

Stimuli-responsive hydrogels respond to changes in their physical and chemical environment. The properties of these materials, including their volume and their mechanical response, can be reversibly controlled by external stimuli such as pH, ion concentration, temperature or electric fields.[1–4, 7] Typical examples of this class of materials are hydrogels or microgels made from the polymer poly(N-isopropylacrylamide) (pNIPAM), which exhibits a lower critical solution temperature (LCST) at around 32°C. Near the LCST, a temperature variation of merely a few degrees can lead to a change in volume by more than an order of magnitude [2–4]. Such a dramatic response to external stimuli can be exploited in applications including stimuli-responsive surfaces [5], soft valves [6], or responsive materials for drug delivery systems [7].

The change in volume is only one manifestation of the alterations in the physical state of the system as the temperature is increased across the LCST; the thermal and the mechanical properties of the material also undergo significant changes. The associated changes in *thermal properties* have been widely investigated in pNIPAM solutions and networks using Differential Scanning Calorimetry (DSC) [8, 9]. Typically, a pronounced endothermic peak corresponding to the LCST is observed in the heat flow. For pNIPAM microgels, alterations of the *mechanical properties* have been investigated using multiple techniques, including conventional mechanical compression tests [10], osmotic compression measurements [11, 12], atomic force microscopy (AFM) [13], and Capillary Micromechanics [14–16]. When the material can be considered elastically homogeneous, Capillary Micromechanics provides experimental access to both the elastic shear modulus G and the compressive elastic modulus K , thus quantifying the full elastic behavior of the

material, including the Poisson’s ratio ν . Using this technique on pNIPAM microgels, a pronounced dip in the Poisson’s ratio was observed around the LCST of these microgels [16], in agreement with previous measurements on macroscopic pNIPAM hydrogels by Hirotsu [17], where an even more dramatic dip was observed. This dip is due to a reduction of the bulk modulus K relative to the shear modulus G , which can be rationalized by considering that the large thermal expansion coefficient near the LCST should intuitively go hand in hand with a large compressibility — the argument being that volume changes, whether thermally or mechanically induced, are less energetically costly in this temperature range. This example illustrates the inherent connection between the thermal and mechanical behavior of these materials.

However, this link has not yet been exploited to extract mechanical properties directly from calorimetric measurements. To achieve this would be especially valuable for determining the mechanical properties of small (sub-micron) particles, or oddly shaped materials, to which standard mechanical measurement techniques are not readily applicable.

In this Letter, we demonstrate that compressive elastic moduli can be determined using DSC measurements, by exploiting the inherent thermodynamic link between calorimetric and mechanical material properties of temperature-sensitive hydrogels. The essence of the method is to compare the energy required to cross the LCST-transition between hydrogels of varying water content (i.e. compression state). Experimentally, we use temperature-responsive poly-N-isopropyl-acrylamide (pNIPAM) based hydrogels as a model material. The difference in energy between compressed (concentrated) and fully swollen gels represents the energy needed to

compress the gels at constant temperature; this energy difference is thus a direct measure of the material's bulk (compressive) elastic modulus. We validate our new calorimetry-based approach by using traditional osmotic compression measurements and find good agreement.

We synthesize our pNIPAM hydrogel samples by mixing 40 mL of Milli-Q water (resistivity $> 18 \text{ M}\Omega\text{cm}$) with 5 wt% NIPAM (N-isopropylacrylamide, Sigma Aldrich), 0.25 wt% cross-linker (Methylene bisacrylamide, Sigma Aldrich) and 0.1 wt% photo-initiator (Irgacure, Sigma Aldrich), corresponding to a monomer to cross-linker weight ratio of 100:5. After shaking, we transfer the solution to a well plate (2mL, VWR) and place it under a UV lamp (Vilber-Lourmat, model VL215.LC, highest intensity, distance $\approx 9 \text{ cm}$) for 1 hour, which results in the formation of a cross-linked pNIPAM gel network. The resulting hydrogels are cut into small pieces, which are then placed in deionized water and allowed to swell overnight. The equilibrium volumes of the hydrogel samples are determined by removing the individual samples from the water bath and weighing them on a microbalance.

As a starting point for the development of our new experimental approach, we first characterize the mechanical properties of the hydrogel samples using a well-established osmotic compression method [18]. This serves both as a validation and as a motivation for the development of our method. In this method, changes in gel volume in response to an applied external osmotic pressure Π_{ext} are measured, yielding the compressive modulus K of the gel.[18]

To this end, we place our samples into dialysis tubes (VWR) and submerge these in dextran solutions ($M_w = 70 \text{ kg/mol}$, Leuconostoc, Sigma-Aldrich) of concentrations ranging from 3.5 wt% to 18 wt%, corresponding to osmotic pressures between 2.28 kPa and 62.5 kPa [18, 19]. We then allow the gels to equilibrate for a period of one week in the dextran solutions, after which their final equilibrium weight is measured. From these data we extract the equilibrium volumes as a function of the applied osmotic pressure, $V(\Pi_{\text{ext}})$. The volume-dependent compressive modulus $K(V)$ is then determined from its definition, $K(V) = - (V/V_0) \frac{\partial \Pi_{\text{ext}}}{\partial (V/V_0)}$, where Π_{ext} is the applied osmotic pressure, and the normalized volume V/V_0 is the ratio of the compressed volume V to the equilibrium, fully swollen volume V_0 . In Fig. 1 the results of the osmotic compression experiments are shown as open circles.

Since obtaining the compressive modulus K from the osmotic pressure curve involves taking a derivative, we want to describe the data using a simple and continuous functional form. To arrive at a physically motivated expression for doing so, we follow the standard scaling arguments for the equilibrium swelling of gels [20], equating the osmotic pressure difference between the semidilute pNIPAM solution and the dextran solution ($\Pi_{\text{ext}}(V)$)

with the elastic modulus of the gel, as

$$\Pi_{\text{ext}} = \beta \left(\frac{V}{V_0} \right)^{-9/4} - \beta \left(\frac{V}{V_0} \right)^{-1/3}. \quad (1)$$

Here, the first term on the right hand side denotes the osmotic pressure of a semidilute polymer solution and the second term represents the elastic modulus according to rubber elasticity. We treat the prefactors as fitting parameters, and because $V = V_0$ at $\Pi_{\text{ext}} = 0$, the two prefactors must be identical, leaving a single fitting parameter β .

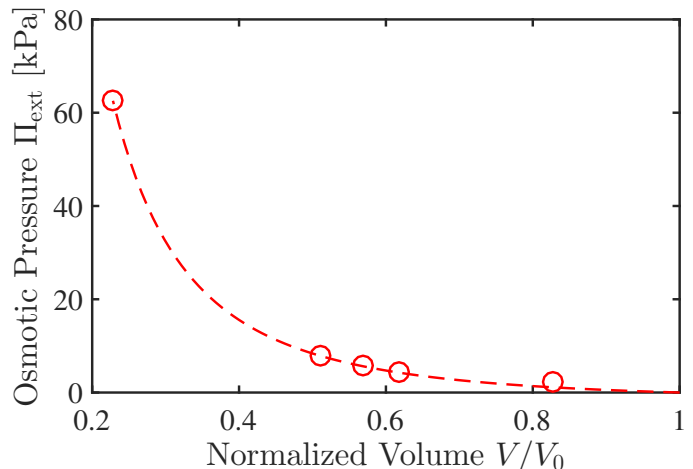


FIG. 1: Osmotic pressure as function of the normalized hydrogel volume V/V_0 . The red circles are the experimental data from the osmotic compression tests and the dashed line is a fit to Eq.(1), with $\beta = 2.39 \pm 0.06 \text{ kPa}$.

This simple, physically motivated, functional form provides a good approximation of the experimental data, as is shown in Fig. 1, where the fit to Eq.(1) is shown as a dashed line. Using this approximation, we extract a compressive modulus as a function of V/V_0 ; at the equilibrium volume, we obtain $K(V_0) \approx 4.59 \pm 0.12 \text{ kPa}$.

From the fitted osmotic compression data (Eq.1) we can also determine the energy $\Delta E(V)$ required to compress the hydrogel from its equilibrium volume V_0 to a compressed volume V . This compression energy is calculated by the integral of the applied pressure difference $\Pi_{\text{ext}}(V)$ over the gel volume, from V_0 to V , as

$$\Delta E(V) = \int_{V_0}^V \Pi_{\text{ext}}(\tilde{V}) d\tilde{V}. \quad (2)$$

Moreover, we note that the compressive modulus K can be determined directly from the energy difference $\Delta E(V)$ via a double derivative, as $K(V) = -V \frac{\partial \Pi_{\text{ext}}}{\partial V} = -V \frac{\partial^2 E}{\partial V^2}$. This brings us to the key element of our method: The difference in energy between a swollen and a compressed state can be determined using calorimetry, without measuring any stresses or pressures, as would be required in

a traditional mechanical test. We illustrate this schematically in Fig. 2A: a gel that is initially swollen and a gel which is initially compressed will end up in the same state (at volume V_f and temperature T_f) when the temperature is increased from T_0 to T_f . The mechanical energy $\Delta E(V)$ used in compressing the gel thus equals the difference between the energies $E(V_0)$ and $E(V)$ that are in turn associated with increasing the temperature of the swollen and the compressed gel samples, respectively.

We implement this idea experimentally by performing DSC runs on the same pNIPAM hydrogels used in the osmotic pressure tests. For these measurements, the gels are prepared in different states of compression, by partial rehydration of dried gels using deionized water. We use the same sample to scan a range of different concentrations, from highly compressed to fully swollen.

The thermodynamic responses are studied using a heat flux Differential Scanning Calorimeter (Q2000, TA instruments). The temperature is increased from 10°C to 55°C at a rate of 0.125°C/min; here, the temperature is held for 10 minutes. The sample is then cooled down to 10°C using the same rate. Again, the sample is held at this temperature for 10 minutes, after which the procedure is repeated once.

The energy required to heat the sample from its initial to its final temperature is determined, using Eq. 2, by calculating the area under the heat capacity curves, as shown in Fig. 2B. The background level of the heat capacity, which is dominated by the heat capacity of water, is subtracted; the data are also normalised by the sample dry weight so that the results for all samples can be directly compared (see Supplementary Material for more details).

We determine $\Delta E(V)$ for hydrogels of different dry weight and at different degrees of compression. The resulting elastic energy of compression, as a function of the volume ratio V/V_0 , is plotted as red triangles in Fig. 3A. We fit these data to the expression obtained from combining Eq. (1) and Eq. (2) resulting in

$$\Delta E(V) = \frac{4\beta}{5} \left(\frac{V}{V_0} \right)^{-5/4} - \frac{3\beta}{2} \left(\frac{V}{V_0} \right)^{2/3} + 0.7\beta, \quad (3)$$

where we have added the term 0.7β to comply with the boundary condition $\Delta E = 0$ at $V = V_0$. The $-5/4$ power is the dominant term in most of the fitting range, and we see in Fig. 3A that the experimental data clearly follows this behaviour, as indicated by the dotted line; this demonstrates that our choice for the functional form for Π_{ext} is appropriate. The corresponding fit to the experimental data is shown as a solid line and for comparison, the dashed line shows the corresponding results using the value of β obtained from the osmotic compression experiment. These results clearly indicate that the two completely different experimental approaches lead to consistent results, thereby confirming the validity of our DSC-

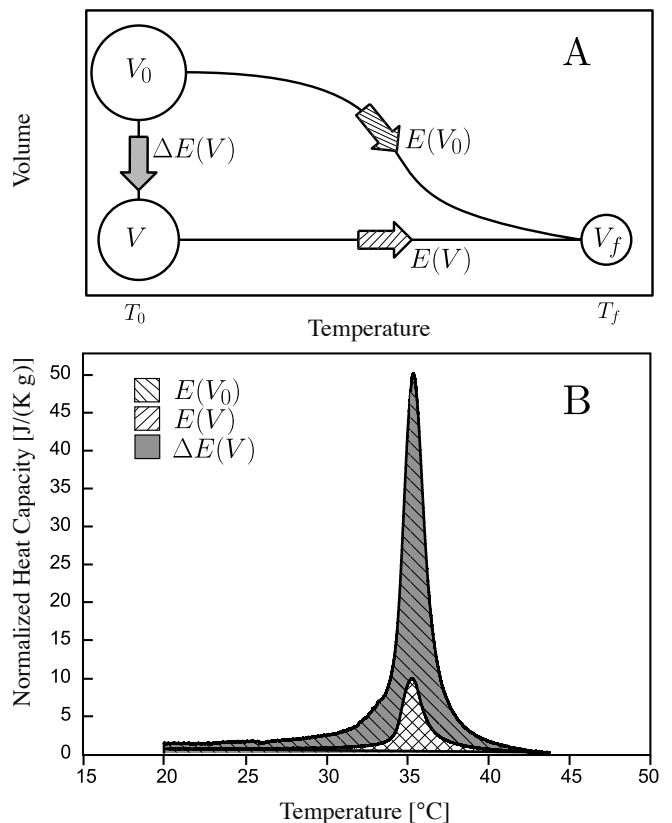


FIG. 2: Extracting mechanical properties from calorimetry. **A)** Schematic phase diagram of calorimetric measurements. An energy of $E(V_0)$ and $E(V)$, for the uncompressed and compressed state, respectively, is required to heat the sample from an initial temperature T_0 to a final temperature T_f . The energy difference $\Delta E(V)$ is the energy required to compress a particle from V_0 to V at a constant temperature. This constitutes a mechanical measurement of the compressive modulus. **B)** Typical corresponding calorimetry measurements: Excess heat capacity per gram of pNIPAM as function of temperature for a compressed (lower curve) and a fully swollen (higher curve) sample; a flat level of heat capacity, dominated by the background water, has been subtracted. We observe a clear peak around the LCST for both samples. The energy under the curves corresponds to the excess energy required to heat the samples, per gram of pNIPAM. Indeed for the uncompressed sample, we find a higher area (---dashed) than for the compressed sample (---dashed). The energy difference (marked as the grey area) corresponds to the mechanical energy $\Delta E(V)$ required to compress the sample from V_0 to V .

based approach. Moreover, from the obtained $\Delta E(V)$ we can calculate the compressive modulus K as a function of V/V_0 via the second derivative of the fitted energy curve; the result is shown in Fig. 3B. In the swollen state, at $V = V_0$, we obtain $K \approx 6.32 \pm 0.24$ kPa, in good agreement with the 4.59 ± 0.12 kPa obtained via the osmotic compression experiment.

In summary, we have performed calorimetric measurements on pNIPAM hydrogels at different levels of com-

pression. We show that the energy required to heat the material to a temperature above the LCST is lower for a compressed than for an uncompressed sample. The difference between these energies represents the energy needed to compress the gels at a constant temperature, which in turn yields the compressive modulus.

To minimize the amplification of experimental errors introduced by the necessary double derivatives, we fit the energy data to a physically meaningful functional form and use this approximation to extract elastic moduli. The compressive modulus obtained using this method is in good agreement with the results from conventional osmotic compression measurements performed on the same gels. We note that to achieve accurate measurements of the compressive modulus, a series of DSC experiments across a significant range of concentrations is required. Moreover, the heating rate in the DSC experiment should be slow enough to give the gels sufficient time to reach equilibrium during de(swelling). As a result, the measurements are relatively time-consuming. However, the sample preparation for the DSC experiments is straightforward and we expect the method to be applicable to a wide range of materials that exhibit a volume phase

transition. Importantly, our results demonstrate that calorimetry can be a powerful technique to determine the mechanical properties of temperature-responsive gels. This can be particularly useful for sub-micron and oddly shaped materials for which established methods are inadequate.

We thank Paul van der Schoot for valuable discussions. The work of FJA and HMW forms part of the research programme of the Dutch Polymer Institute (DPI), project 738; we are grateful for their financial support. JM and HMW are also grateful to the Royal Society (IE111253) for financial support.

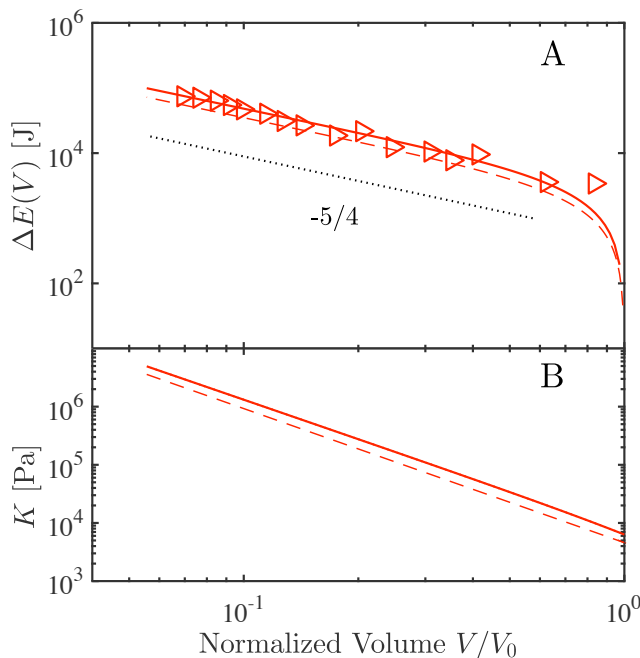


FIG. 3: **A)** Compression Energy $\Delta E(V)$ as function of the volume ratio V/V_0 . The red triangles are the calorimetric results and the solid line is the fit using Eq. (3) resulting in $\beta \approx 3.29$ kPa. This is in good agreement with the prediction based on the osmotic compression measurement, plotted as a dashed line. The dotted line indicates a slope of $-5/4$ which is the dominant term in Eq. (2). **B)** Corresponding compressive modulus K as function of V/V_0 . At $V = V_0$ we find $K = 6.32 \pm 0.24$ kPa and 4.59 ± 0.12 kPa based on DSC and osmotic compression, respectively.

-
- * Electronic address: H.M.Wyss@tue.nl
- [1] S. Y. Kim and Y. M. Lee, *Journal of Applied Polymer Science* **74**, 1752 (1999), ISSN 1097-4628.
 - [2] J. Wu, B. Zhou, and Z. Hu, *Physical Review Letters* **90**, 48304 (2003).
 - [3] B. R. Saunders and B. Vincent, *J. Chem. Soc. Faraday Trans.* **92**, 3385 (1996).
 - [4] L. Arleth, X. H. Xia, R. P. Hjelm, J. Z. Wu, and Z. B. Hu, *Journal of Polymer Science Part B-Polymer Physics* **43**, 849 (2005).
 - [5] X. Liu, Q. Ye, B. Yu, Y. Liang, W. Liu, and F. Zhou, *Langmuir* **26**, 12377 (2010).
 - [6] C.-H. Zhu, Y. Lu, J. Peng, J.-F. Chen, and S.-H. Yu, *Advanced Functional Materials* **22**, 4017 (2012).
 - [7] A. Yamazaki, F. Winnik, R. Cornelius, and J. Brash, *Biochimica et Biophysica Acta - Biomembranes* **1421**, 103 (1999).
 - [8] Y. Yan, L. Huang, Q. Zhang, and H. Zhou, *Journal of Applied Polymer Science* **132** (2015), ISSN 1097-4628.
 - [9] F. Afroze, E. Nies, and H. Berghmans, *Journal of Molecular Structure* **554**, 55 (2000), ISSN 0022-2860.
 - [10] M. Yuan, X. Ju, R. Xie, W. Wang, and L. Chu, *Particulology* **19**, 164 (2015), ISSN 1674-2001.
 - [11] B. Sierra-Martín, Y. Laporte, A. B. South, L. A. Lyon, and A. Fernández-Nieves, *Phys. Rev. E* **84**, 011406 (2011).
 - [12] B. Sierra-Martin, J. A. Frederick, Y. Laporte, G. Markou, J. J. Lietor-Santos, and A. Fernandez-Nieves, *Colloid and Polymer Science* **289**, 721 (2011).
 - [13] S. M. Hashmi and E. R. Dufresne, *Soft Matter* **5**, 3682 (2009).
 - [14] H. M. Wyss, T. Franke, E. Mele, and D. A. Weitz, *Soft Matter* **6**, 4550 (2010).
 - [15] M. Guo and H. M. Wyss, *Macromol. Mater. Eng.* **296**, 223 (2011).
 - [16] P. Voudouris, D. Florea, P. van der Schoot, and H. M. Wyss, *Soft Matter* **9**, 7158 (2013).
 - [17] S. Hirotsu, *Macromolecules* **23**, 903 (1990).
 - [18] A. Fernandez-Nieves, A. Fernandez-Barbero, B. Vincent, and F. J. de Las Nieves, *J Chem Phys* **119**, 10383 (2003).
 - [19] B. Sierra-Martin, J. A. Frederick, Y. Laporte, G. Markou, J. J. Lietor-Santos, and A. Fernandez-Nieves, *Colloid and Polymer Science* **289**, 721 (2011).
 - [20] M. Rubinstein and R. H. Colby, *Polymer physics* (2003).

SUPPLEMENTARY MATERIAL: ANALYSIS OF DIFFERENTIAL SCANNING CALORIMETRY (DSC) MEASUREMENTS

The measured heat capacities for pNIPAM hydrogels of various states of compression are shifted with respect to each other due to different amounts of water in the gel and the three different amounts of dry weight of pNIPAM hydrogel samples used ($10.3 \mu\text{g}$, $12.2 \mu\text{g}$ and $20.9 \mu\text{g}$), this can be seen in Fig 4. In order to compare the data, we have to correct for the dry weight and the amount of water. In the temperature range that we are interested in the heat capacity of water is essentially a flat line, as seen in Fig 4 (0 wt% solid line with open circles). At $T=55^\circ\text{C}$, the material should have reached its final volume V_f and we expect the signal to be predominantly due to the water background. Thus, by subtracting the value of the heat capacity at $T=55^\circ\text{C}$, we can correct the data for the variation in water content. The result of this subtraction is plotted in Fig. 5.

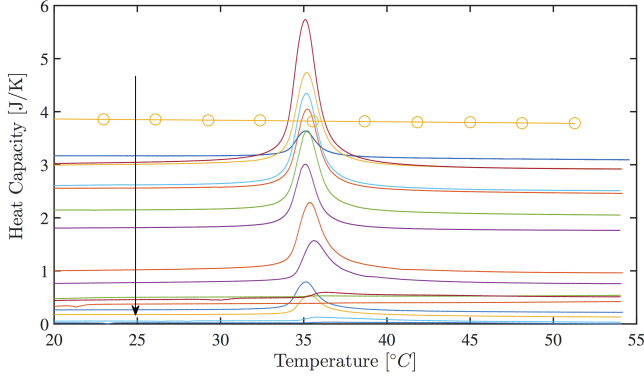


FIG. 4: Measured heat capacity as function of temperature for the hydrogel samples at different dry weights of pNIPAM. The solid line shows data for the $10.3 \mu\text{g}$ sample, the dashed line for the $12.2 \mu\text{g}$ and the dotted line for the $20.9 \mu\text{g}$. The solid line with open circles is a pure water sample of $504 \mu\text{g}$. In the direction of the arrow the sample concentrations are: 0, 5, 20, 11.9, 14, 11.2, 13.3, 12.6, 55, 65, 75, 85, 95, 60, 80, 90 wt%.

Because we use hydrogel samples with three different pNIPAM dry weights ($10.3 \mu\text{g}$, $12.2 \mu\text{g}$ and $20.9 \mu\text{g}$), we also need to normalize each type of sample by its dry weight in order to compare samples at the same state of compression but containing different amounts of pNIPAM. The resulting specific heat capacity or weight normalized heat capacity is shown in Fig. 6. The top curve represents the DSC run for the fully swollen hydrogel

and the area under this curve is $E(V_0)$. By subtracting the areas under the other curves $E(V)$ from this value, the compression energies $\Delta E(V)$ can be determined for different degrees of compression. For clarification in the same graph the pure water sample is shown (solid line with open circles). This curve is normalized with the weight of the water, because the dry weight of pNIPAM is 0 in this case.

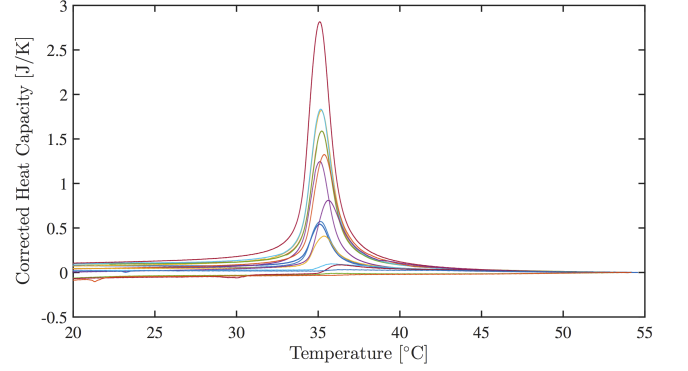


FIG. 5: Corrected heat capacity as function of temperature for the samples at different dry weights of pNIPAM. The solid line is for the $10.3 \mu\text{g}$ sample, the dashed line for the $12.2 \mu\text{g}$. The color coding is the same as in Fig. 4

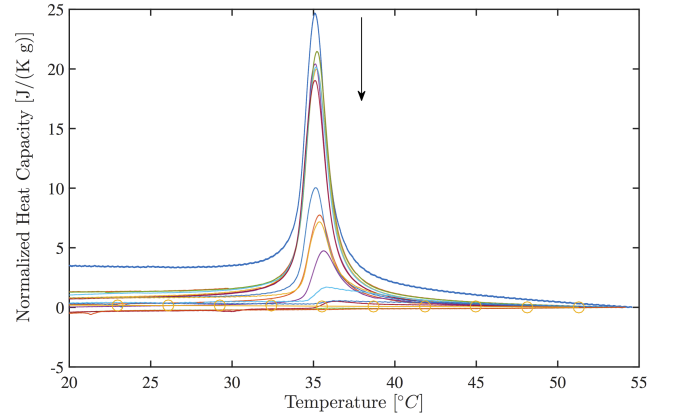


FIG. 6: Corrected heat capacity normalized by the dry weight of pNIPAM as a function of temperature. The solid line is for the $10.3 \mu\text{g}$ sample, the dashed line for the $12.2 \mu\text{g}$. The solid line with the open circles is the shifted heat capacity of the water normalised by its weight. The color coding is the same as in Fig. 4. The exact order of concentrations in direction of the arrow is: 5, 11.2, 13.3, 12.6, 14, 11.9, 55, 50, 85, 60, 65, 80, 90, 0, 85, 75, 95 wt%. The order is not exactly as expected.